A Virtual Reality Based System for Relics Restoration

Norihiro Abe[1], Yasuhiro Watanabe[1], Kazuaki Tanaka[1],
Jiangyu Zheng[1], Shoujie He[2], Hirokazu Taki[3],
Yoshimasa Kinoshita[4], and Akira Yokota[4]

[1]Dept of Mechanical Systems Engineering,
[2]Dept of Computer Science and Electronics,
Faculty of Computer Science and Systems Engineering
Kyushu Institute of Technology
Kawazu 680-4, Iizuka, Fukuoka 820-8502, JAPAN
[3]Mitsubishi Electronic Inc., JAPAN
[4]Dept of Neurosurgery, School of Medicine
University of Occupational and Environmental Health
Yahatanishi-ku, Kitakyushu 807, JAPAN
hesj@cse.kyutech.ac.jp

Abstract

Most of the relics dug out so far are found in fragments. For the purpose of study, analysis, and display, it is always necessary to restore the relics from the fragments. The restoration, however, is a hard task. The adhesive agent used may damage the fragments and the restoration process is usually irreversible. This paper presents a virtual reality based restoration method, which enables us to restore the relics in a virtual environment without using the fragments in the real world. The virtual fragments are obtained by measuring the 3D data of the real fragments with the MRI (Magnetic Resonance Imaging) technology. This paper describes the MRI data acquisition, the conversion from the MRI data to polygon data, the 3D construction of the virtual fragments, and the procedure for the restoration of the relics in the virtual environment.

Key words: Virtual Reality, 3D restoration of relics from fragments, MRI, HMD, Data Glove

1. Introduction

Most of the relics dug out so far are found in small fragments. For the purpose of studying and analyzing the culture and technologies at the time when the relics were created and also for the display of the relics in a museum, it is required to restore the relics from the fragments.

Conventionally, restoration operations are directly applied to the fragments. Because an adhesive agent is often used to hold a pair of supposedly adjacent fragments together, it is normally impossible to get back the original individual fragments once they have been glued together. Moreover, the restoration from the fragments is usually very complicated and a trial and error process is unavoidable. Therefore, the conventional restoration operations unavoidably cause damage to the fragments. Besides, once the relics has been restored, the individual fragments can never be examined anymore.

With the advancement of 3D measurement technologies, it becomes possible to measure with high accuracy the 3D data of an object. With the drastic progress of computer hardware technologies, virtual reality as a new enabling technology is drawing more and more attention. In a virtual environment, we can dynamically change our viewpoint and interactively work with the virtual object through translation, rotation, and scaling operations.

This paper presents a virtual reality based restoration system, which enables us to restore the relics in a virtual environment without using the fragments in the real world. The restoration process consists of three steps, 3D measurement of the fragments, construction of the virtual fragments, and restoration of the relics from the virtual fragments. The details of the three steps are described in Sections 2, 3, and 4, respectively. Experimental results are shown in Section 5.

2. 3D Measurement of the Fragments

MRI technology is used to measure the 3D data of the fragments. One of the merits of using the MRI technology is that both sides of the fragments can be measured at the same time and with high accuracy. The demerit, on the other hand, is that inorganic substance such as the fragments of the relics has no response to

the MRI signals and thus it is difficult to directly measure the 3D data of the fragments. In order to overcome the difficulty, we sink the fragments in agaragar jelly.

We use a 10 cm x 10 cm x 10 cm container to contain the agaragar jelly. This enables us to measure the 3D data of the whole set of the fragments at the same time. In addition, no matter how complicated the shape of the fragments might be, the measurement is always with high accuracy. In order to have a noise free measurement results as much as possible, we put quite a few types of drugs such as gadolinium into the jelly.

The principle of the MRI measurement is to generate a set of cross section images of the container with an adjustable interval. In this research, the interval is set to be 0.5 mm based on the tradeoff between the measurement time and modeling accuracy. Therefore, totally we get 200 cross section images. Among the cross section images, only those including the cross sections of the fragments are considered. The details of the MRI measurement technologies can be found in Ref.[1].

3. Construction of the Virtual Fragments

As mentioned in Section 2, the data measured with the MRI device are simply a set of cross section images (MRI images) of the fragments. In order to construct the 3D model of the fragments, we need to process the MRI images so that the information necessary for the 3D model generation can easily be obtained.

3.1 Preprocessing to the MRI images

The MRI images are gray scale images and the responses of the agaragar jelly to the MRI signal are not very uniform although the uniformity has been improved by the drugs mixed up. However, since the fragments have no response to the MRI signal, the corresponding regions are extremely dark. It is, therefore, easy to find an appropriate threshold for the extraction of the fragment regions. Figure 1 shows an MRI image and its binarized image. The binarization threshold is automatically detected by the method described in Ref. [2].

The MRI image in Fig. 1 contains the cross sections from two different fragments. It is also possible that the cross sections from two or more different parts of the same fragment together with the cross sections from the other fragments appear in the same MRI image. For the convenience of the construction of the 3D model from the cross sections, we assign a specific label to each of the fragment regions. The labeling processing is based on the spatial connectivity among the pixels [3]. After the labeling processing, a boundary detection operator is used to detect the boundaries of the connected components. The boundary detection operator is as follows:

$$B(x, y) = \begin{cases} 0 & \text{if } I(x-1, y) = I(x+1, y) = I(x, y-1) = I(x, y+1) \\ 1 & \text{otherwise} \end{cases}$$

where I(x, y) denotes a pixel on the binarized image and B(x, y) denotes its counterpart on the boundary image. Note that the above operator is only applied to the pixels belonging to the fragment regions, i.e., I(x, y) = 1. Figure 2 shows the boundary image of the binarized image in Fig. 1 (b).

3.2 3D model generation

In principle, the boundary data of the cross sections can directly be used to construct the 3D surface model of the fragments. Moreover, it is true that a very fine 3D model will be generated if all the points on the boundary are used. However, the 3D model generated will be very heavy to manipulate unless an extremely fast workstation is used. For this reason, we take the following steps to obtain a vectorization representation of the boundaries.

Step 1: Track a boundary and compute the local curvature for each of the boundary points. Let `E[k]` denote a boundary point with `0 <= k <= N-1`, where N is the total number of the boundary points. Initialize `E[0]`, the start point for the vectorization, with the boundary point having the largest curvature. In the case that more than one boundary points have the same largest curvature, the one first tracked is assigned to `E[0]` by default. Since the vectorization will go through the whole set of boundary points and terminates at the start point `E[0]`. The terminator, `T`, is set to be `E[0]`, as well.

Step 2: Use the following procedure to find `E[n]` and then use the vector from `E[0]` to `E[n]` to represent the boundary segment from `E[0]` through `E[n]`.

```
n = 1;
do {
   n = n + 1;
   th = f(n); // f(n): evaluation function
} while( th < TH );
                  // TH: a pre-set threshold
vector( E[0], E[n] );
```

where $f(n)=\Sigma d^2[k]$ with `k = 1, ..., n` and `d[k]` is the distance from `E[k]` to the straight line that `E[0]` and `E[n]` are on.

Step 3: If `E[n] != T` then set `E[0] = E[n]` and go back to step 2; otherwise, terminate the vectorization process.

The pre-set **TH** value is very critical. A large **TH** may refine the boundary with less boundary points and thus the polygon generated at the later stage will be easy to manipulate. The boundary points dropped out, however, may correspond to the shape details useful for the judgement of adjacency with other fragments. A small **TH**, on the other hand, may not improve the manipulatability of the virtual fragment sufficiently.

Next to the vectorization of the boundaries is the generation of 3D surface model of the fragment slices. This can be done simply by incorporating the thickness of the slices. The thickness information can be obtained from the interval with which the MRI images are generated. The interval is 0.5 mm which corresponds to about two pixels on an image. Therefore, the 3D model of the slices are generated simply by adding the thickness of 2 pixels along the direction perpendicular to the image plane.

Finally, we construct the virtual fragments by piling the slices up. The label information and the 2D location of the slices are used to guide the construction process.

4. Relics Restoration from the Virtual Fragments

Figure 3 shows the organization of our restoration system. With the data glove, magnetic sensor, and the HMD (Head Mounted Display), manipulating the virtual fragments in the virtual environment is as if we are operating on the real objects in the real world. In Fig. 3, the data glove is used to detect whether the operator has bent his first or his second joint of his fingers. In response to the bending situation, the system on the workstation will decide whether to pick up a virtual fragment or not. The magnetic sensor is used to detect the 3D location of the data glove. Only when the data glove is close enough to a virtual fragment, can we pick up the fragment by bending our fingers. HMD is used to monitor the virtual space and the restoration operations.

A 3D model of the data glove is generated in the virtual space. Whether a virtual fragment should be picked up is judged by detecting the interference between the polygons of the fragment and the polygons of the data glove model. For a better visualization effect, once a fragment has been picked up, the system will not display the data glove model. If the interference happened between a fragment and the data glove model, the fragment is picked up and will follow the movement of the operator's hand. Releasing a fragment is done by bending a pre-determined finger.

Since we have only one data glove, we cannot hold a pair of fragments at the same time as we do in the real world. In order to overcome this difficulty, we set up a separate virtual space, which is dedicated for the restoration operations. Once a fragment is released in the restoration space, the fragment will be fixed at the location where it is released. Since we can change our viewpoint to the restoration space as we like, we can start from any fragment but normally starting from a relatively big fragment is advised. The restoration procedure is as follows:

Step 1: Pick up a big fragment and release it in the restoration space.

Step 2: Choose the fragment from the remainders and check whether it is adjacent to the one in the restoration space. In oder to correctly judge the adjacency, we may need to repeat the picking up and releasing operations to change the grasping position. We may change our viewpoint to the virtual space where the fragments are stacked so that the times of the repetition between picking up and releasing is reduced.

Step 3: Repeat Step 2 until no fragment left.

5. Experimental Results

Figure 4 is a china jar, which is used in our experiment. Figure 5 shows the fragments of the jar. Totally 20 fragments are obtained. Figure 6 shows the whole set of the virtual fragments, which are constructed from the MRI images. Figure 7 (a) shows the fragment constructed with all the boundary points. Figure 7 (b) shows the fragment constructed after vectorizing the boundaries. Figure 8 is a different viewpoint to the fragments in Fig. 7. It can be seen that shape details useful for the judgement of the adjacency with other fragments are kept quite well. The data size of the vectorization representation is only one tenth of the original one. Considering the number of the fragments, we can see how important it is to generate the vectorization representation.

Following the restoration procedure described in Section 4, we finally restore a virtual jar from the virtual fragments. Figure 9 show the restored jar from four different viewpoints.

Because the accurate data of both sides of the fragments can be obtained with MRI devices, we also tried with the interpolation for the case that some fragments are missing. The interpolation is based on the curvature information of the surrounding fragments. Figure 10 shows the result that we successfully interpolate the missing fragments.

6. Concluding Remarks

A virtual reality based approach to the relics restoration has been presented. Restoration operations including

the trial and error process are all done in a virtual environment and hence no damage to the real fragments is caused. Once the correct adjacency relationships are discovered by a skilled operator, we may train a novice to learn the expertise and know-how simply by repeating the restoration steps.

MRI measurement technology is still under improvement. With the shortened measurement time, we may set a smaller interval for the cross section image acquisition and thus a more accurate model will be generated. In addition, boundary vectorization can be further improved by incorporating ideas of the scale space filtering [4]. The reduction of the boundary points is contradictory with the accuracy of the restoration. This is because the adjacency between a pair of fragments is judged based on the detailed shape feature of the boundary. A better choice for the boundary vectorization might be to fit with a straight line the relatively smooth boundary segments, while keeping the boundary segments with frequent changes not fitted at all.

In addition to the shape features, the textures on the surface of the fragments are also very important to the judgement of the adjacency between a pair of fragments. One of our future work is to map the texture on the surface of the virtual fragments to improve the virtual restoration performance.

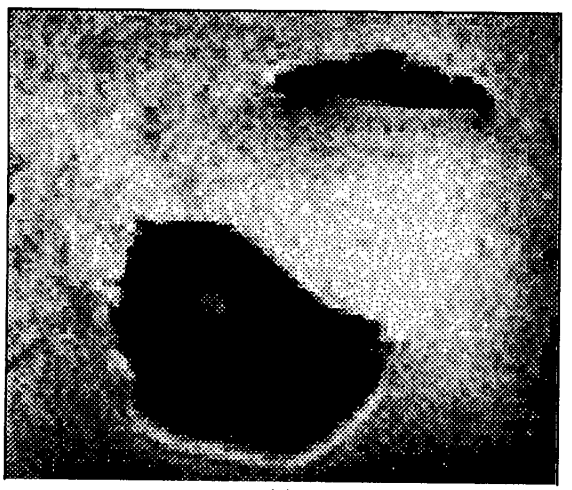

(a)

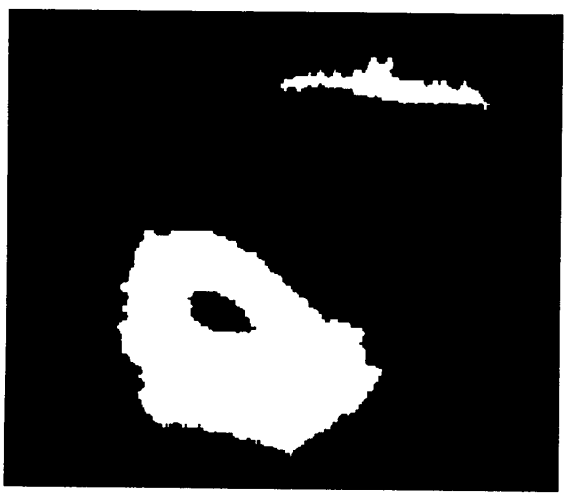

(b)

Figure 1: (a) an MRI image, (b) its binarized image.

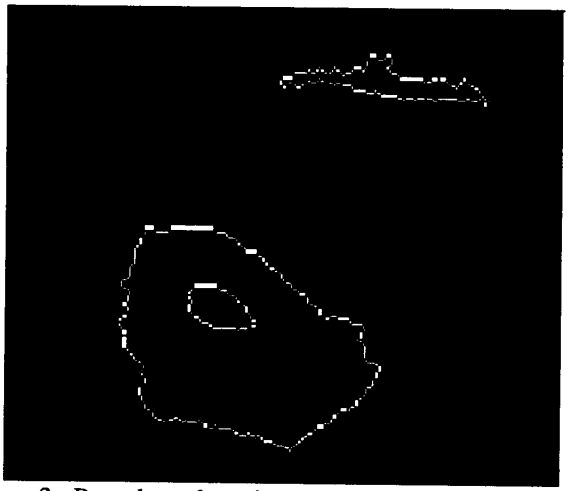

Figure 2: Boundary detection results of the image in Fig. 1(b).

References

1. Y. Kinoshita et al., "User Manual for Magnetic Resonance Instrument", Journal of the University of Occupational and Environmental Health, 16(4), pp. 301-308, 1994.

2. N. Otsu, "A threshold selection method from gray level histograms", IEEE Trans. Systems Man Cybernet. 9, pp. 62-66, 1979.

3. A. Rosenfeld et al., Digital Picture Processing, Volume 2, Academic Press, 1987.

4. A. Pentland, From Pixels to Predicates, Chapter 1, Ablex Publishing, 1986.

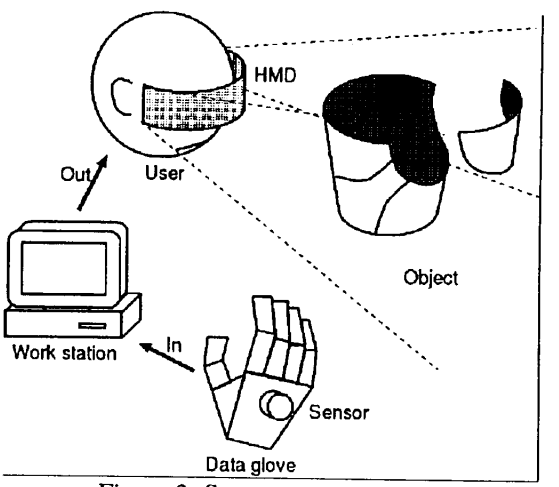

Figure 3: System organization.

Figure 4: A china jar used in our experiment.

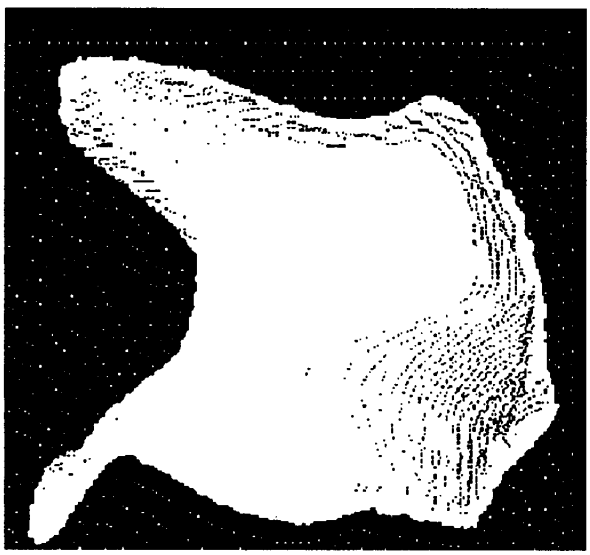

(a)

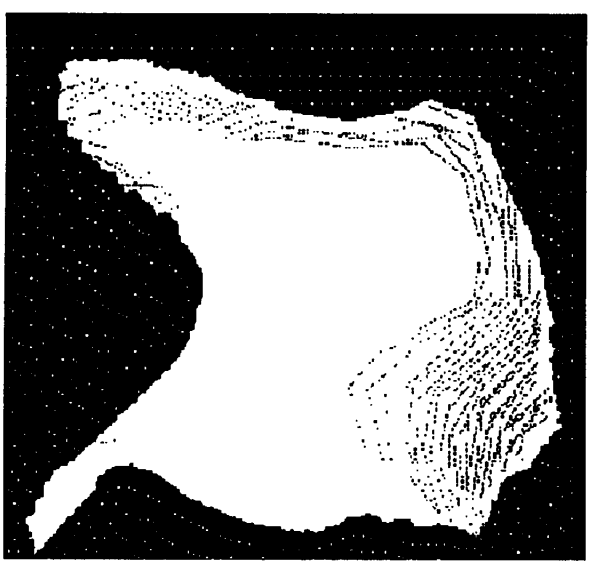

(b)

Figure 7: A fragment constructed from (a) the original boundary points (b) the vectorized boundary points.

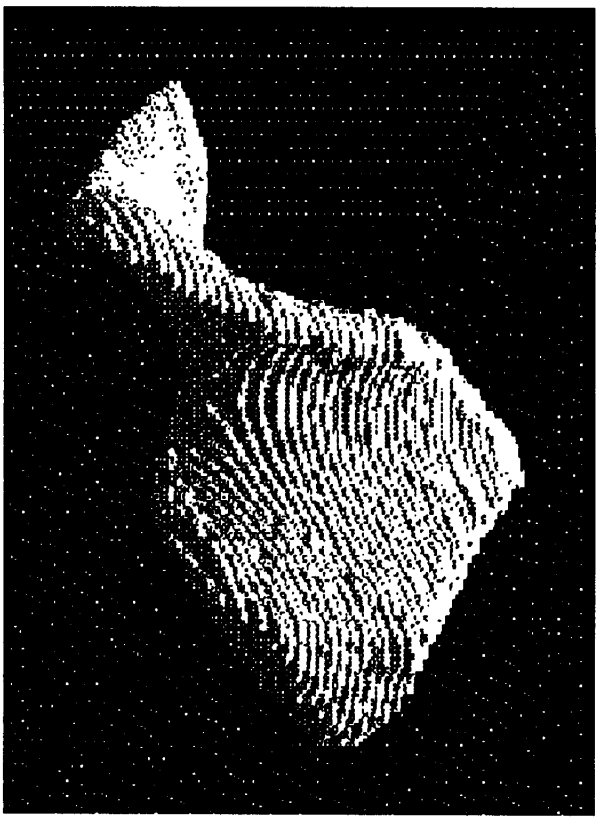

(a)

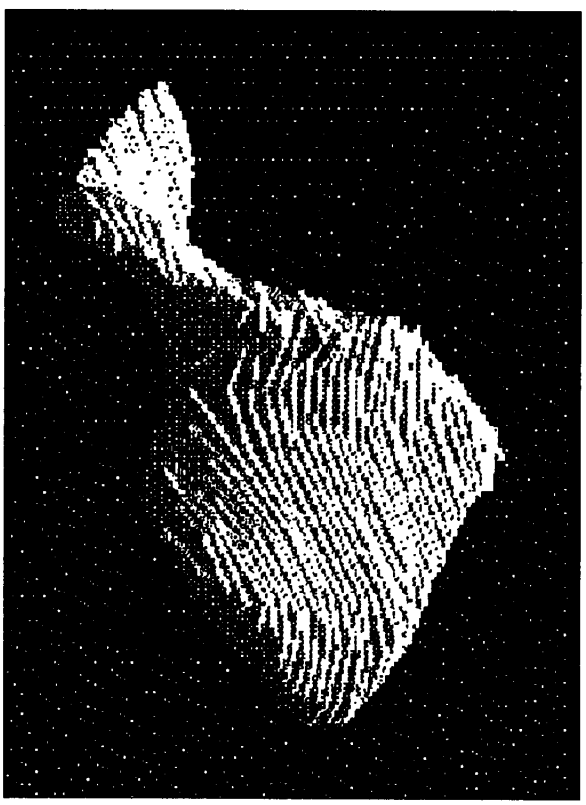

(b)

Figure 8: A different view of the fragment shown in Fig. 7. (a) and (b).

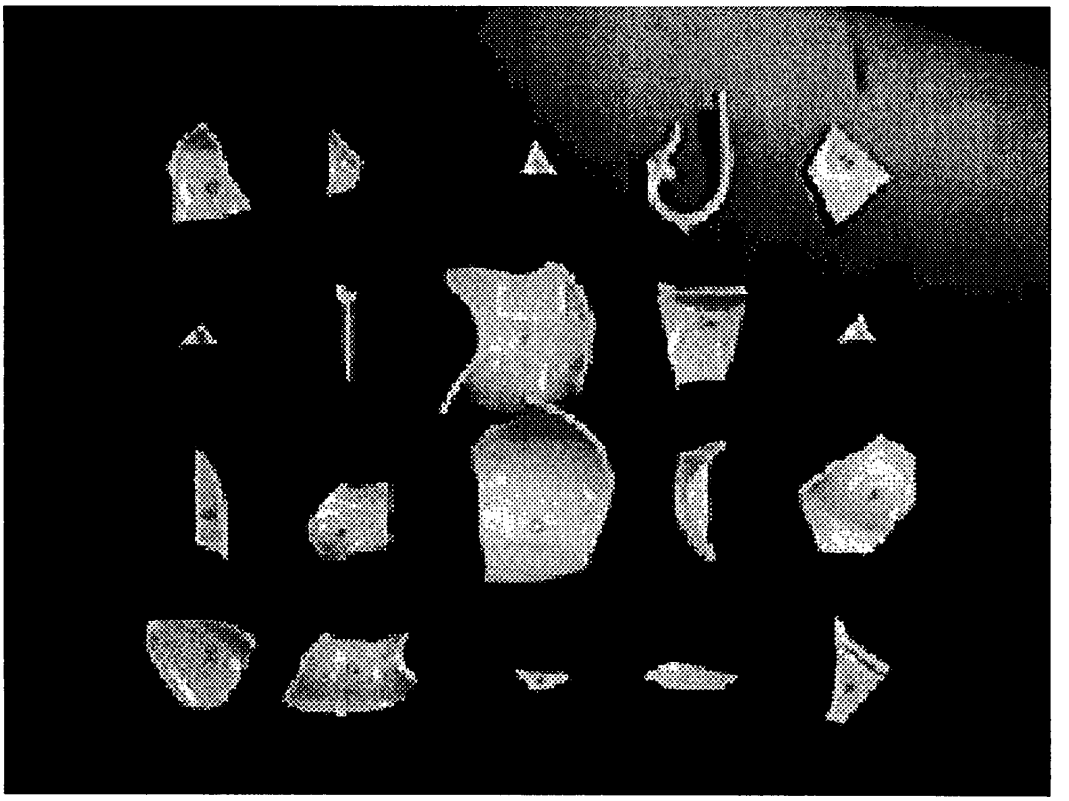

Figure 5: Totally 20 fragments are obtained.

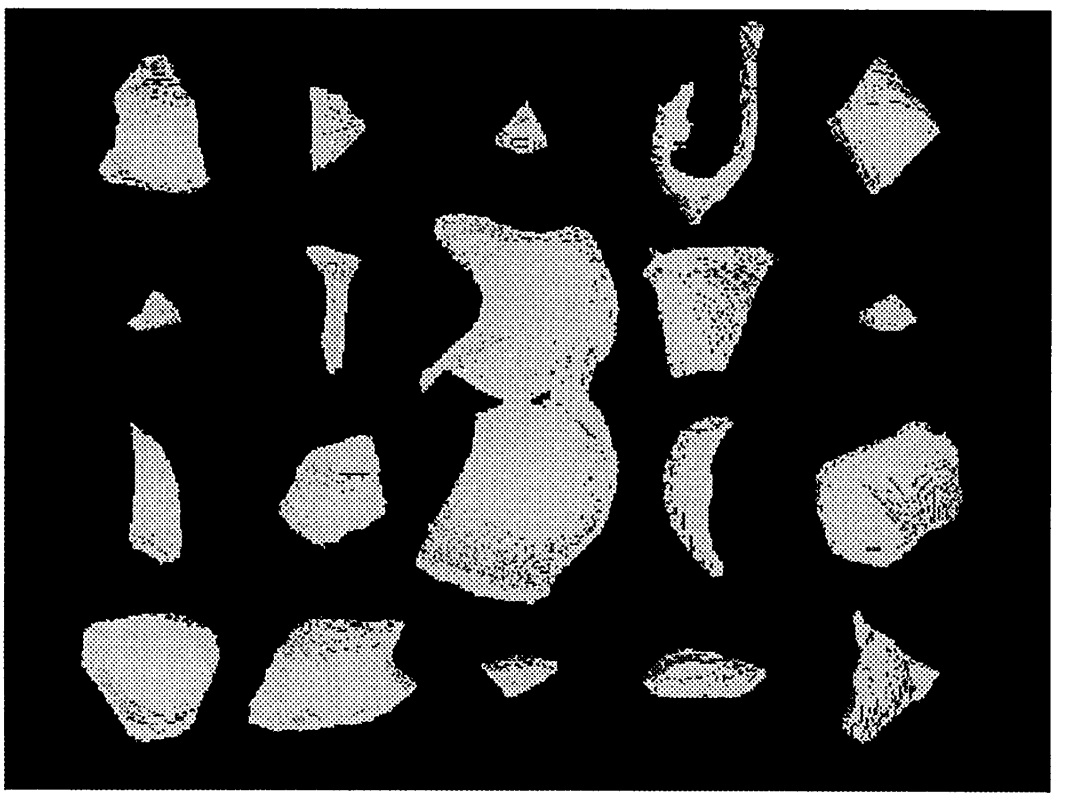

Figure 6: Totally 20 virtual fragments are constructed from the MRI images.

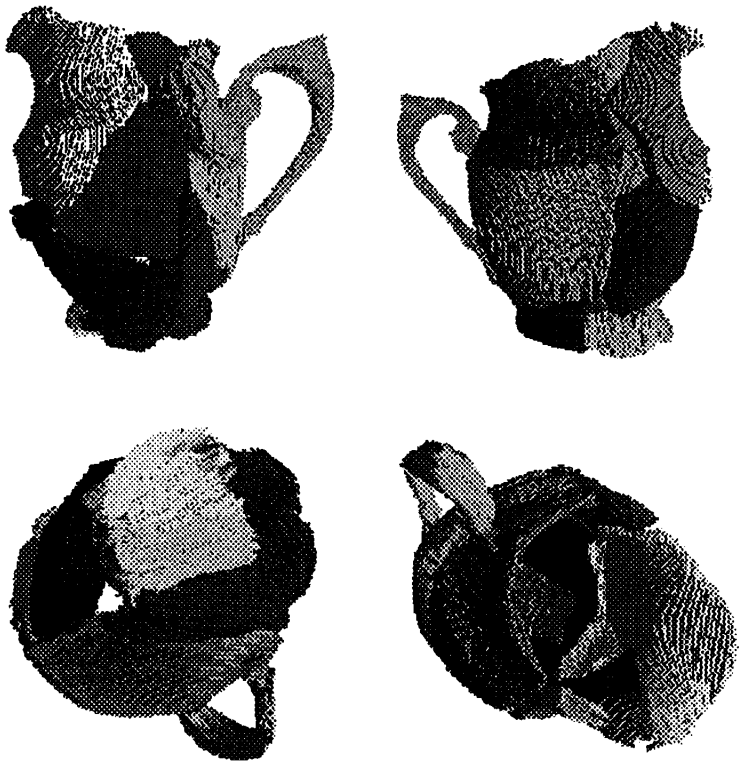

Figure 9: Four different views of the restored jar.

Figure 10: The restoration results of the jar, where the missing fragment has been interpolated.